Purinergic Signalling (2024) 20:521–532
https://doi.org/10.1007/s11302-023-09984-5

RESEARCH

Limited contribution of the of P2X4 receptor to LPS-induced microglial reaction in mice

Nobili Paola[1,2] · **Ulmann Lauriane**[1,2] · **Rassendren François**[1,2] · **Hirbec Hélène**[1,2]

Received: 10 August 2023 / Accepted: 12 December 2023 / Published online: 30 December 2023
© The Author(s), under exclusive licence to Springer Nature B.V. 2023

Abstract

Sepsis is life-threatening condition that can trigger long-term neurological sequelae, including cognitive impairment in survivors. The pathogenesis of the so-called sickness behavior is poorly understood, but sepsis-driven neuroinflammation is thought to play a key role. Microglia are the central nervous system resident immune cells and play major roles in the induction and the control of neuroinflammatory processes. Accordingly, we recently demonstrated important microglia reaction, characterized by dramatic microglia transcriptome remodeling, in an experimental model of sepsis. Interfering with microglia pathways thus represents an interesting opportunity to tune microglia reaction towards beneficial outcomes. Purinergic signaling is central to microglia biology and controls key microglia functions. In particular, P2X4 receptors, which are highly permeable to calcium and de novo expressed in reactive microglia, seem to be an interesting target to modulate microglia reaction. Here, we investigated the impact of P2X4 receptors on the LPS-driven microglia transcriptome remodeling. Although we used complementary and sensitive biostatistical approaches, we did not measure significant impact of P2X4 deficiency onto microglia transcriptome either in homeostatic nor reactive condition. Overall, our results revealed that microglia reaction elicited by LPS-mediated sepsis is P2X4 independent and highlights the functional diversity of microglia reaction. These results also promote for the search of disease-specific targets to tune microglia reaction towards beneficial outcomes.

Keywords Microglia · Transcriptome · RNAseq · Lipopolysaccharide (LPS) · P2rX4

Introduction

Sepsis is a life-threatening multiorgan dysfunction arising from dysregulated response to infection. Clinical signs are diverse but generally include respiratory failure, shock and fever [1]. The central effects of sepsis are known for a long time but were initially thought to be caused by pathogens themselves. However, studies have revealed that the sepsis-driven sickness behavior mainly results from a central response to peripherically released cytokines produced by immune cells and tissue resident macrophages [2–4]. In the context of infection, sickness behavior is beneficial as it leads to nutriment restriction that in return limits the replication of pathogens. However, it can also affect neuropsychological functions such as learning and memory, especially when infection is intense and/or prolonged.

Microglia are the main immuno-competent cells of the central nervous system and play many key functions both under physiological and physio-pathological conditions (for review [5]). In particular, in response to perturbations of the nervous system homeostasis, microglia become reactive. Microglia reaction is a complex and not so well understood mechanism. Recent studies revealed that reactive microglia exist in multiple states that likely drive different microglial functions which can be either beneficial or deleterious for brain activities [6]. Yet, the role of microglia in the induction and the maintenance of the sickness behavior remains poorly understood. In this context, we have previously shown that the microglia transcriptome is acutely dramatically altered in an experimental model of sepsis based on the systemic administration of a high dose of lipopolysaccharide (LPS), an endotoxin from Gram$^-$ bacteria [7]. This suggests that microglia are critically involved in this syndrome and opens

Rassendren François and Hirbec Hélène contributed equally to the work.

✉ Hirbec Hélène
helene.hirbec@igf.cnrs.fr

[1] Institute of Functional Genomics, CNRS, INSERM, University of Montpellier, Montpellier, France

[2] Labex ICST, Montpellier, France

the way to modulate microglia reaction addressing it towards beneficial effects.

Microglia express a large repertoire of purinergic receptors, and purinergic signaling is central to microglia biology both in physiological and disease conditions [2, 3]. Purinergic receptors expression is highly dependent on microglia state. Thus, *P2ry12* and *P2ry13* metabotropic receptors are among the most expressed genes in homeostatic microglia, but are strongly down-regulated in reactive states [7]. Conversely, P2X4 receptor (P2rx4), an ATP-gated channel, is virtually absent from homeostatic microglia but up-regulated in reactive microglia [8, 9]. Interestingly, each purinergic receptor controls specific microglia functions. For example, P2ry12 is involved in microglia processes motility [10], whereas P2rx4 is involved in inflammatory processes [11]. As a consequence of this switch in purinergic signaling, reactive microglia loose or acquire specific functions. In neuropathic pain models, de novo P2rX4 expression in spinal microglia has been shown to enhance local network excitability [8, 12]. Similarly, following status epilepticus, P2rx4 expressing hippocampal microglia have been shown to contribute to microglial-evoked neuroinflammation and neuronal death [13]. Further, in a mouse model of Alzheimer disease (AD), our group recently showed that genetic blockade of *P2rX4* is accompanied by a reduction of soluble $A\beta_{1-42}$ peptide level and a reversal of cognitive deficits [14]. However, to our knowledge, the contribution of P2X4 receptors to neurological conditions characterized by strong neuroinflammation but lack of neurodegeneration, as is the case during sepsis, has not been studied.

Here, building on our previous study [7], we performed whole transcriptome profiling of purified cortical microglia from individual adult mice to investigate the extent to which P2X4 receptors expression contributed to the microglial transcriptome in a model of sepsis. Using a wide range of complementary bioinformatic approaches, we characterized the impact of *P2rX4* on the repertoire of genes expressed by microglia in both physiological conditions and in a model of peripheral sepsis, induced by intraperitoneal administration of LPS.

Materials and methods

Animals, LPS treatments

In this study, we used female $CX3CR1^{+/GFP}$ and $P2X4^{-/-}{:}CX3CR1^{+/GFP}$ mice aged 60–80 days (C57BL6/J background). Generation of $CX3CR1^{+/GFP}$ [15] and $P2X4^{-/-}{:}CX3CR1^{+/GFP}$ is described in [8, 16]. For simplification $CX3CR1^{+/GFP}$ and $P2X4^{-/-}{:}CX3CR1^{+/GFP}$ mice are thereafter referred to as $P2X4^{+/+}$ and $P2X4^{-/-}$ mice respectively. Mice were bred in our IGF animal facility that holds an institutional license approved by the French Ministry of Agriculture (N° D34-172–13). They were housed in a 12 h light–dark schedule with food and water ad libitum. All experiments followed European Union (Council directive 86/609EEC) and institutional guidelines for the care and use of laboratory animals. The animal experiment protocols used in this study were approved by the Comité d'Ethique pour l'Expérimentation Animale Languedoc Roussillon (CEEA-LR; APAFiS#5253).

LPS administration To induce a neuroinflammatory reaction, a dose of 4 mg/kg of LPS (*Escherichia coli* 026; #L2654; Sigma-Aldrich, Lyon, France) diluted in PBS was intraperitoneally (i.p.) injected. Control mice received an i.p. injection of PBS. Mouse body weights were measured just before and 24 h after i.p. injection. Mice were euthanized 24 h after i.p. administration.

Tissue collection

Tissue collection and preparation After induction of deep anesthesia with 2 µg/g pentobarbital (Euthasol Vet, TVM), mice were perfused intracardially with 10 ml of phosphate buffer saline (PBS). For gene expression studies, the cortex was dissected, immediately frozen and stored at − 80 °C until use. For histological studies, the brains were fixed with 4% paraformaldehyde (PFA, Sigma-Aldrich, P6148) for 2 h at room temperature (RT) and then overnight at 4 °C in fresh 4% PFA. Fixed brains were stored at 4 °C in PBS containing 0.1% sodium azide until they were cut into 40 µm sections using a Vibratome (Microm Microtec, Brignais, France).

Immunohistochemistry, image acquisition and quantification

Vibratome floating sections were incubated overnight at 4 °C with the appropriate primary antibody: Rabbit-IBA1 (1:2000, Wako, MNK4428) diluted in 2% BSA, 0.1% Triton X-100, PBS solution. Sections were then rinsed 3 times with PBS and incubated for 2 h at RT with Goat anti-Rabbit Cy3 secondary antibody (1:500, Jackson, 111–165-144). After a final rinsing session, sections were then mounted using Dako Fluorescent Mounting Medium (Dako, S3023) and stored at 4 °C until imaging.

Slides were viewed using a classical epifluorescence microscope, and images were acquired using an Imager Z1 microscope (Zeiss) equipped with an AxioCam MR R3 camera under a 20X/0.50 M27 Zeiss Plan-Neofluar air objectives. IBA1 staining was quantified by acquiring, for each field, 11 images (corresponding to 10-µm-thick optical sections). All images were acquired with the same exposure time. Stacked images were projected on the Z-axis and analyzed using a custom ImageJ macro to determine the

percentage of immunopositive surface. For each animal, quantifications were performed in four to five randomly selected fields per section with at least five sections per animal. Three (PBS injected) and five (LPS injected) mice were analyzed.

Microglia isolation

The procedure to isolate microglia from brain is described in details in [7]. After induction of deep anesthesia, mice were perfused intracardially with 10 ml of PBS. The cortex was dissected and mechanically homogenized in Hank's Balanced Salt Solution containing 0.6% glucose and 15 mM HEPES using a glass-teflon dounce homogenizer. After filtration through a 70 µm cell strainer the cell suspension is mixed in 1:3 proportions with a 100% Percoll solution. The resulting 75% Percoll solution was then overlaid with 25% Percoll solution and further with PBS. The gradients were then centrifuged at 4 °C for 25 min at 800 g in swinging buckets. After centrifugation, the top layer containing myelin and debris (interface PBS/25% Percoll) was removed, and the cellular layer at the 25%/75% interphase was collected and washed by a series of centrifugation/resuspension steps. The final pellet was resuspended in PBS and subjected to flow cytometry. Microglia sorting was performed at the Montpellier Rio Imaging (MRI) Core Facility at the Institute for Regenerative Medicine and Biotherapy (IRMB, Montpellier) using a FacsAria (BD Biosciences) cell sorter. Microglia cells were sorted following the gating scheme presented in Fig. 1A. Sorted cells were GFP^{++} events from which doublets were eliminated. Characterization of GFP^{++} isolated cells was described in details in [7]. In brief, isolated cells were 99% pure, showed homogeneous size and granularity, had intermediate CD45 and CD11b expression and were $CD4^{-}$, $CD8^{-}$ and $MHCII^{-}$. The isolation process, from dissection to final sorting, lasted between 3.5 and 4 h. Sorted cells were directly collected in RLT buffer (Qiagen), and lysates were frozen and stored at − 80 °C until total RNA extraction.

RNA isolation and RNA-Seq

Total RNA was extracted from sorted microglial cells using the RNeasy micro kit (Qiagen). All RNAs samples were treated with DNase I according to the manufacturer's recommendations. The quality of the total RNA was checked using the Agilent 2100 Bioanalyzer (Agilent). All RNAs had RNA Integrity Numbers (RINs) higher than 8.0. Five individual replicates per experimental condition were used.

Library preparation and RNA sequencing were performed by the ProfileXpert core facility (Lyon, France). cDNAs were synthetized and amplified (12 cycles) from 5 ng of DNase-treated total-RNA using the SMARTer™ Ultra Low RNA kit for Illumina sequencing (Clontech). Library preparation was performed using the Ovation ultralow kit (NuGEN) according to the manufacturer's instructions. Libraries were sequenced using an Illumina HiSeq2500 platform, and 50 bp single-end sequencing data was obtained with approximately 20–26 million reads passing filters per sample.

Reads were aligned to the mouse genome (GRCm38 mm10) with a set of gene model annotations (i.e. genes.gtf downloaded from UCSC on May 23 2014; GeneIDs come from the NCBI: gene2refseq.gz downloaded on September 14 2015) using the CRAC software [17]. In mean 21 million reads were mapped to the genome. The featureCounts tool was used to determine the number of reads mapping to each gene [18]. Between 11.5 and 15.3 (13.6 ± 1.3) million reads were mapped on genes. Before normalization and statistical analysis, genes with less than 12 reads in at least 5 samples were filtered out.

Bioinformatics analyses

Differential gene expression Samples to be included in the different analyses were selected according to the question addressed. After selection, gene expression normalization was performed using Relative Log Expression (RLE) normalization implemented in the EdgeR 3.8.6 R package [19]. Generalized Linear Models (GLM) with tagwise dispersion was applied to detect the differentially expressed genes (DEG) depending on either the genotype ($P2X4^{-/-}$ vs $P2X4^{+/+}$) or the treatment (LPS vs PBS). Fold-change, *p* value and False Discovery Rate (FDR) were computed. Counts per million mapped reads (Cpm) were also determined.

Principal component analysis (PCA) was performed using FactoMiner R package [20].

Functional and pathways enrichment analysis To study the biological mechanisms and gene ontology associated with DEG, we used the g:Profiler software (https://biit.cs.ut.ee/gprofiler/gost). For these analyses, Gene Ontology (GO)-biological processes associated with the selected genes were listed; nodes (GO-biological process) with adjusted *p* value less than 5% were reported as important. Kyoto Encyclopedia Gene and Genomes (KEGG [21]) and Reactome [22] databases were also used to perform pathway enrichment analyses. To avoid overly specific and general processes, only processes with between 30 and 300 genes were considered.

Gene set enrichment analysis (GSEA) [23] was performed on all 10,778 expressed genes using the Cpm values obtained from EdgeR as expression values. GSEA analyses were run for either control or LPS-treated samples, comparing

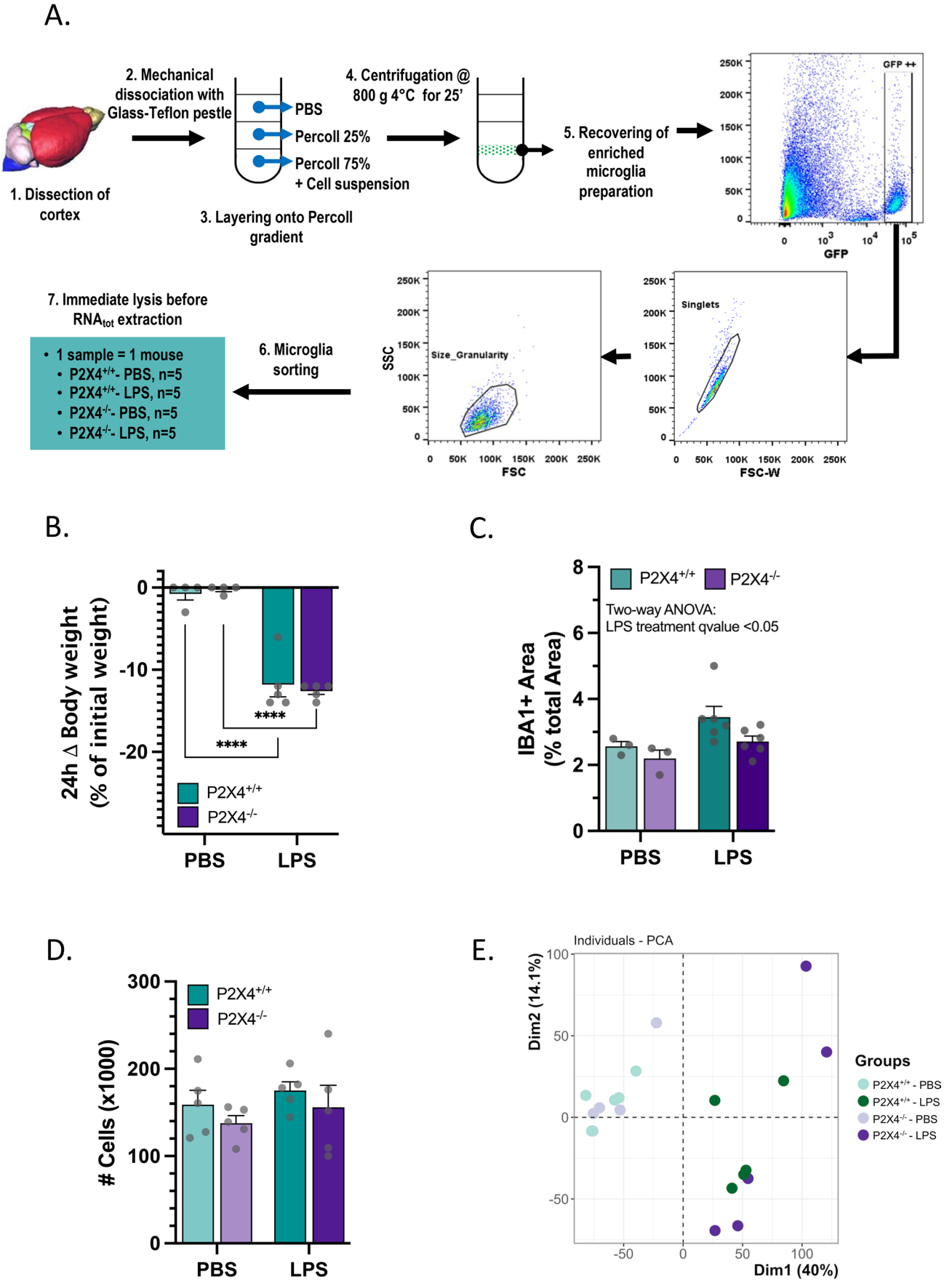
A.
1. Dissection of cortex
2. Mechanical dissociation with Glass-Teflon pestle
3. Layering onto Percoll gradient
PBS
Percoll 25%
Percoll 75%
+ Cell suspension
4. Centrifugation @ 800 g 4°C for 25'
5. Recovering of enriched microglia preparation
GFP ++
GFP
Singlets
Size_Granularity
SSC
FSC
FSC-W
6. Microglia sorting
7. Immediate lysis before RNAtot extraction
• 1 sample = 1 mouse
• P2X4+/+- PBS, n=5
• P2X4+/+- LPS, n=5
• P2X4-/- PBS, n=5
• P2X4-/- LPS, n=5
B.
24h Δ Body weight (% of initial weight)
P2X4+/+
P2X4-/-
****
****
PBS
LPS
C.
IBA1+ Area (% total Area)
Two-way ANOVA:
LPS treatment qvalue <0.05
PBS
LPS
D.
Cells (x1000)
PBS
LPS
E.
Individuals - PCA
Dim2 (14.1%)
Dim1 (40%)
Groups
P2X4+/+ - PBS
P2X4+/+ - LPS
P2X4-/- - PBS
P2X4-/- - LPS

◂**Fig. 1** Microglia isolation procedure and overall effects of LPS administration. **A**. Schematic overview of microglia sorting procedures. Percoll gradient-isolated leukocytes from control and LPS-injected CX3CR1$^{+/egfp}$ mice were gated based on high GFP expression (GFP++). After elimination of the doublets and further refinement based on cell size (Forward Scatter, FSC) and granularity (Side Scatter, SSC), the sorted cells were immediately lysed before RNA extraction and RNA-seq. **B**. Body weight loss measured 24 h after i.p. administration of 4 mg/kg LPS in P2X4$^{+/+}$ and P2X4$^{-/-}$ mice treated with either PBS (light colors) or LPS (dark colors). Statistics: two-way ANOVA with LPS-Treatment and Genotype as between subjects' factors LPS-treatment: $p < 0.001$; FDR corrected post hoc tests LPS vs PBS: **** $p < 0.0001$. Data are mean ± SEM. **C**. Quantification of cortical IBA1 positive area (in % of total area) in P2X4$^{+/+}$ and P2X4$^{-/-}$ mice treated with either PBS or LPS. Statistics: two-way ANOVA with LPS-Treatment and Genotype as between subjects' factors; LPS-treatment: $p < 0.05$. Data are Mean ± SEM. **D**. Number of microglia cells sorted in each experimental condition. E Principal component analysis of gene expression in P2X4$^{+/+}$ and P2X4$^{-/-}$ homeostatic or reactive microglia, based on the 10,788 expressed genes

microglia isolated from *P2X4*$^{+/+}$ and *P2X4*$^{-/-}$ mice respectively. GSEA was conducted with the GSEA software (http://software.broadinstitute.org/gsea/index.jsp). GSEA analyses were performed on gene sets from the Mouse MSigDB Collections (https://www.gsea-msigdb.org/gsea/msigdb/mouse/collections.jsp). Namely, we interrogated gene sets of (1) MH mouse-orthololog hallmark; (2) M2 canonical pathways; (3) M3 Regulatory target and (4) M5 Biological pathways gene sets. Parameters for GSEA were set to include gene sets with between 15 and 200 genes to avoid overly specific or general terms. As recommended in the GSEA user guide, enrichment gene sets with an FDR (q value) < 25% were considered relevant as they are more likely to generate interesting hypotheses and drive further research. However, we also reported enrichment gene sets with an uncorrected p value lower than 1%.

qPCR

Reverse transcription of 500 ng amplified RNA (cell sorted samples) or total RNA (whole cortex samples) was performed using an iScript kit (BioRad). Real-time PCR was performed in 384-well plates in a final volume of 10 µl using SYBR Green dye detection on the LightCycler480 system (Roche-Diagnostic). The primers pairs were designed using Primer 3 software. Lists of genes analyzed and primers sequences/references are given in Table S1. The results were expressed as Cq and normalized to the Cq value of the microglia *Hexb* housekeeping gene (cell sorted samples) or *Ddx17* (whole cortex samples). Normalized values are reported as ($-\Delta$Cq).

Statistics

All data are presented as mean ± standard error of the mean (SEM). They were analyzed using two-way analysis of variance (ANOVA) in GraphPad Prism (9.0) to determine significant main effects and interactions. Post hoc analyses for multiple comparisons were performed with Benjamini, Krieger and Yekutieli False Discovery Rate (FDR) corrections.

Results

P2rX4 deficiency had no global impact on LPS-mediated sickness behavior

Peripheral immune challenges are known to lead to a wide range of effects such as anorexia, anhedonia, decreased activity and metabolic changes. Body weight loss can be used as an integrative parameter of all the above-mentioned effects and is useful to compare the intensity of sickness behavior in different experimental conditions [24]. To evaluate if *P2rx4* deficiency had an overall impact on the development of the sickness response in mice, we injected *P2X4*$^{+/+}$ and *P2X4*$^{-/-}$ adult (≈ 3-month-old) female mice intraperitoneally with LPS and measured their body weight loss 24 h later. As previously described [24], we observed a significant weight loss in *P2X4*$^{+/+}$ animals ($-11.8 \pm 3.5\%$; q value < 0.001; Fig. 1B). Body weight loss in *P2rX4*-deficient mice was also significant ($-12.6 \pm 3.5\%$; q value < 0.001; Fig. 1B) but not different from that in *P2X4*$^{+/+}$, indicating no overall behavioral contribution of *P2rX4* to sickness response in adult female mice.

Transcriptome analysis to assess the contribution of microglial *P2rX4* to LPS-induced inflammatory response

Peripheral immune challenges induce a central reaction characterized notably by a complex microglial reaction that is known to play a key role in the establishment of the neuroinflammatory response. To determine if *P2rX4* has an overall impact on microgliosis, we first quantified the LPS-induced increase in IBA1 staining. Figure 1C revealed that 4 m/kg LPS administration induced an overall increase in the IBA1^{+} surface (Treatment fixed effect: p value < 0.05; two-way ANOVA), but with no significant impact of the genotype (Genotype fixed effect: p value > 0.05; two-way ANOVA). Next, to establish whether *P2rx4* deficiency may affect the LPS-induced microglial reaction at the molecular level, we used a flow cytometry approach to isolate microglia from

both *P2X4*$^{+/+}$ or *P2X4*$^{-/-}$ mice that received either LPS or PBS [7]. The number of microglial cells recovered was about 150 thousand cells per cortex (156 ± 8.2 [100 – 240]) and was similar in all the experimental conditions (Fig. 1D). As in our original experiment, mouse samples were sequenced individually. In total, we identified 10,778 genes expressed in at least five of the 20 microglial samples. Expression values for all expressed genes are reported in Table S1a. Comparison of gene expression profiles among individuals within a same experimental group revealed strong correlation within both the *P2X4*$^{+/+}$ and *P2X4*$^{-/-}$ control groups (*P2X4*$^{+/+}$: $r = 0.984 \pm 0.003$; *P2X4*$^{-/-}$: $r = 0.981 \pm 0.003$). Slightly lower correlation was measured within the LPS-treated samples (*P2X4*$^{+/+}$: $r = 0.961 \pm 0.006$; *P2X4*$^{-/-}$: $r = 0.916 \pm 0.014$). This likely reflects inter-individual treatment-response variability, which appears more pronounced in *P2rX4*-deficient mice (LPS-*P2X4*$^{+/+}$ *vs* LPS-*P2X4*$^{-/-}$: p value = 0.008). The higher interindividual variability among LPS-treated samples, especially in *P2rX4*-deficient mice, is also highlighted in the principal component analysis (PCA) with all samples and expressed genes (Fig. 1E). Overall, the high correlation within each of our experimental groups ensures that transcriptomic remodeling is not masked by interindividual variability.

Lack of *P2rX4* only weakly affects microglia transcriptome in homeostatic conditions

As an initial step towards deciphering the contribution of the P2X4 receptor to the microglial reaction induced by peripheral immune challenge, we evaluated whether *P2rx4* deficiency affects the microglial transcriptome in homeostatic condition. Thus, we compared genes expression in control microglia isolated from the cortex of either *P2X4*$^{+/+}$ or *P2X4*$^{-/-}$ mice injected with PBS.

Both PCA analysis (Fig. 2A) and unsupervised hierarchical clustering (Fig. 2B) on all expressed genes failed to segregate *P2X4*$^{-/-}$ from *P2X4*$^{+/+}$ control microglia suggesting that, under homeostatic conditions, P2X4 receptor deficiency had minor impact on the microglia transcriptome. To go further, we performed differential expression analysis to search for differentially expressed genes (DEG). We identified only 11 DEG with FDR < 0.05, among which six were up-regulated and five down-regulated (including *P2rx4*) (Fig. 2C). Of note, among those *Capn11*, *Ccnb2*, *Oasl1* and *Slc15a2* were only weakly expressed in microglia (i.e. cpm-WT-PBS < 10, Table S1b) and are thus unlikely to play major roles in these cells. Down-regulation of the expression of *Ubc*, *P2rX7* and *Ccdc62* in sorted microglia was confirmed by qPCR (Sup-Fig. 1A–C). Interestingly and consistently with its preferential expression in microglia [25] (https://www.brainrnaseq.org/), *Ubc* down-regulation was also demonstrated in cortical samples (Sup-Fig-1E). Finally, to identify whether the DEG were functionally related, we performed functional analysis using gProfiler. We interrogated several databases, namely GO-Biological processes, KEEG-pathways and Wiki-pathways, but could not associate these 11 genes to any specific pathway or process.

Although differential expression is the gold standard in transcriptomic analyses, it only captures abrupt changes in gene expression. Gene Set Enrichment Analysis (GSEA) is an alternative computational method that determines whether an a priori defined set of genes shows statistically significant concordant differences between two biological states [23]. Interestingly, GSEA uses all expressed genes making it possible to detect situations where all genes in a predefined set change in a small, but coordinated way. This is important for functional analysis as it is likely that many relevant phenotypic differences are manifested by small but consistent changes in a set of genes. Here, we performed GSEA analyses using all expressed genes and comparing *P2X4*$^{-/-}$ to *P2X4*$^{+/+}$ control microglia. We analyzed a wide range of gene sets of the Mouse MSigDB Collections (see materials and methods) and only identified a weak enrichment of the Reactome "Opioid signalling pathway", the Biocarta "HCMV pathway" and the "Chemokine signalling wikipathway" in *P2X4*$^{-/-}$ homeostatic microglia (FDR < 0.25; see detailed results in Table S2). Our analysis also revealed an enrichment for genes predicted to be targets of miR_1843b_5p in *P2X4*$^{-/-}$ microglia. Overall, however, these results as well as those of clustering and differential expression analyses indicated that P2X4 receptor deficiency has only minor effect on microglia biology in homeostatic conditions.

Microglia transcriptome remodeling is minimally affected by *P2rx4* deficiency

To analyze the contribution of P2X4 to sepsis-induced microglia reaction, we then compared gene expression in microglia isolated from the cortex of either *P2X4*$^{+/+}$ or *P2X4*$^{-/-}$ mice injected with 4 mg/kg LPS.

Both PCA analysis (Fig. 3A) and unsupervised hierarchical clustering (Fig. 3B) failed to segregate *P2X4*$^{-/-}$ from *P2X4*$^{+/+}$ LPS-treated microglia suggesting that P2X4 receptor deficiency had no strong impact on LPS-induced microglia remodeling. However, to investigate further and analyze whether P2X4 impacted only on very specific pathways, we performed differential expression analysis to identify DEGs. Because of the slightly higher interindividual variability among experimental groups and because PCA had revealed little impact of the genotype, we reduced the stringency of our analysis and applied a cutoff of 0.1 (instead of 0.05 in homeostatic conditions) for the FDR. Even with these more relaxed conditions, we identified only six DEG, among which one was up-regulated and five

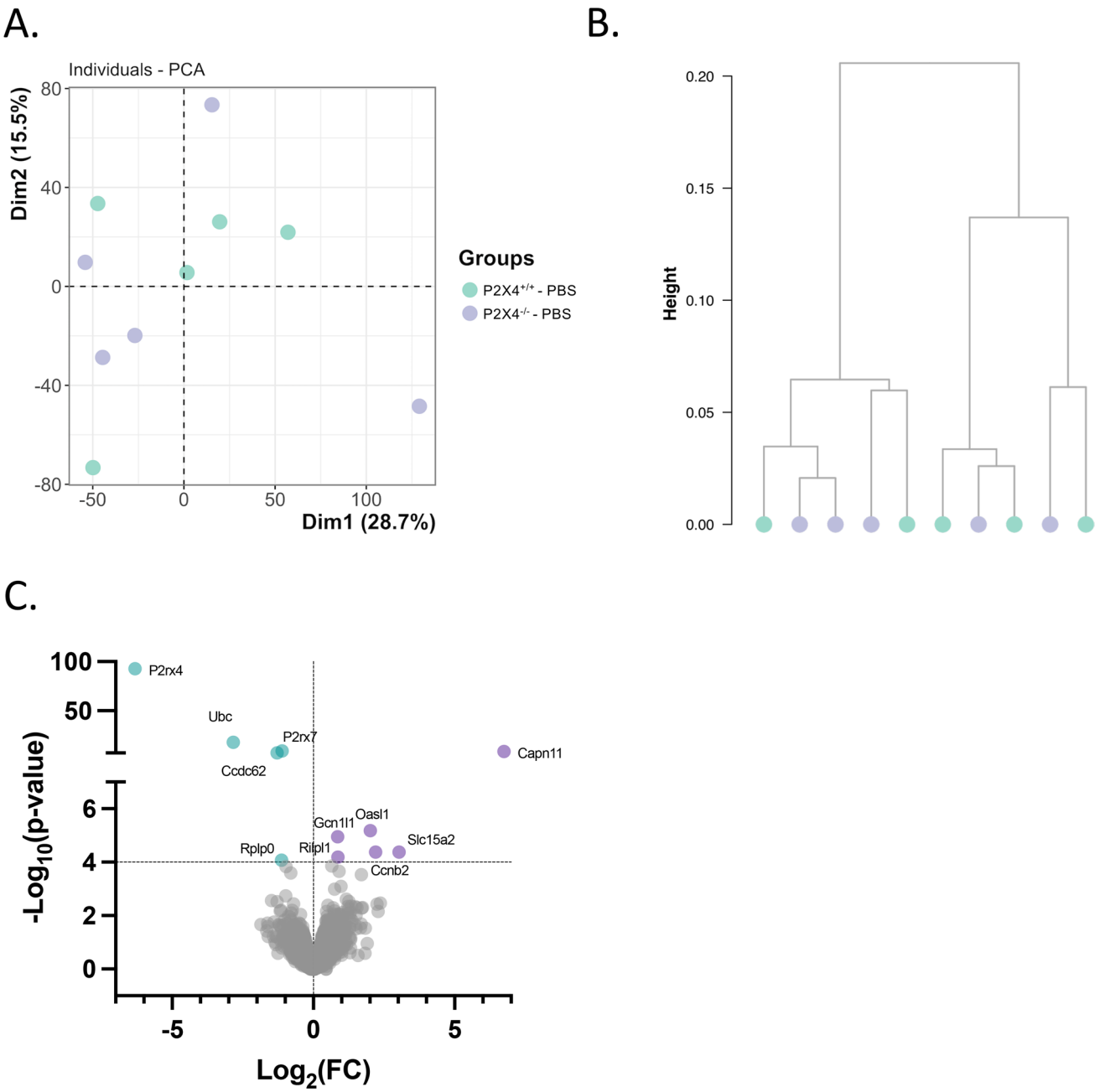

Fig. 2 Impact of *P2rx4* deficiency in homeostatic microglia. **A**. Principal component analysis of gene expression in $P2X4^{+/+}$ and $P2X4^{-/-}$ homeostatic microglia, based on the 10,788 expressed genes. **B**. Hierarchical clustering of gene expression in $P2X4^{+/+}$ and $P2X4^{-/-}$ homeostatic microglia, based on the 10,788 expressed genes. **C**. Volcano plot displaying the 11 genes that are deregulated (FDR < 0.05) in $P2X4^{-/-}$ compared to $P2X4^{+/+}$ homeostatic microglia. x-axis: log2 of fold-change in expression between $P2X4^{+/+}$ and $P2X4^{-/-}$ reactive microglia. y-axis: $-\log_{10}$ of p value; the horizontal dotted line represents a p value $= 10^{-4}$, corresponding to FDR = 0.1. Light green: down-regulated in $P2X4^{-/-}$ Light purple: up-regulated in $P2X4^{-/-}$

down-regulated (including *P2rx4*) (Fig. 3C). From these genes only *Anapc5* up-regulation appears P2X4-dependent (sup-Fig. 1D and Table S1b). We then performed functional analysis on the DEG using gProfiler to determine whether the DEG were functionally related. Despite querying several databases (i.e. GO-Biological processes, KEEG-pathways and Wiki-pathways) reporting thousands of pathways and biological functions, we were unable to associate the DEGs with any specific pathway or process.

To identify whether P2X4 may impact on many genes associated to a specific process or pathway, but with each gene of this process/pathway making only small

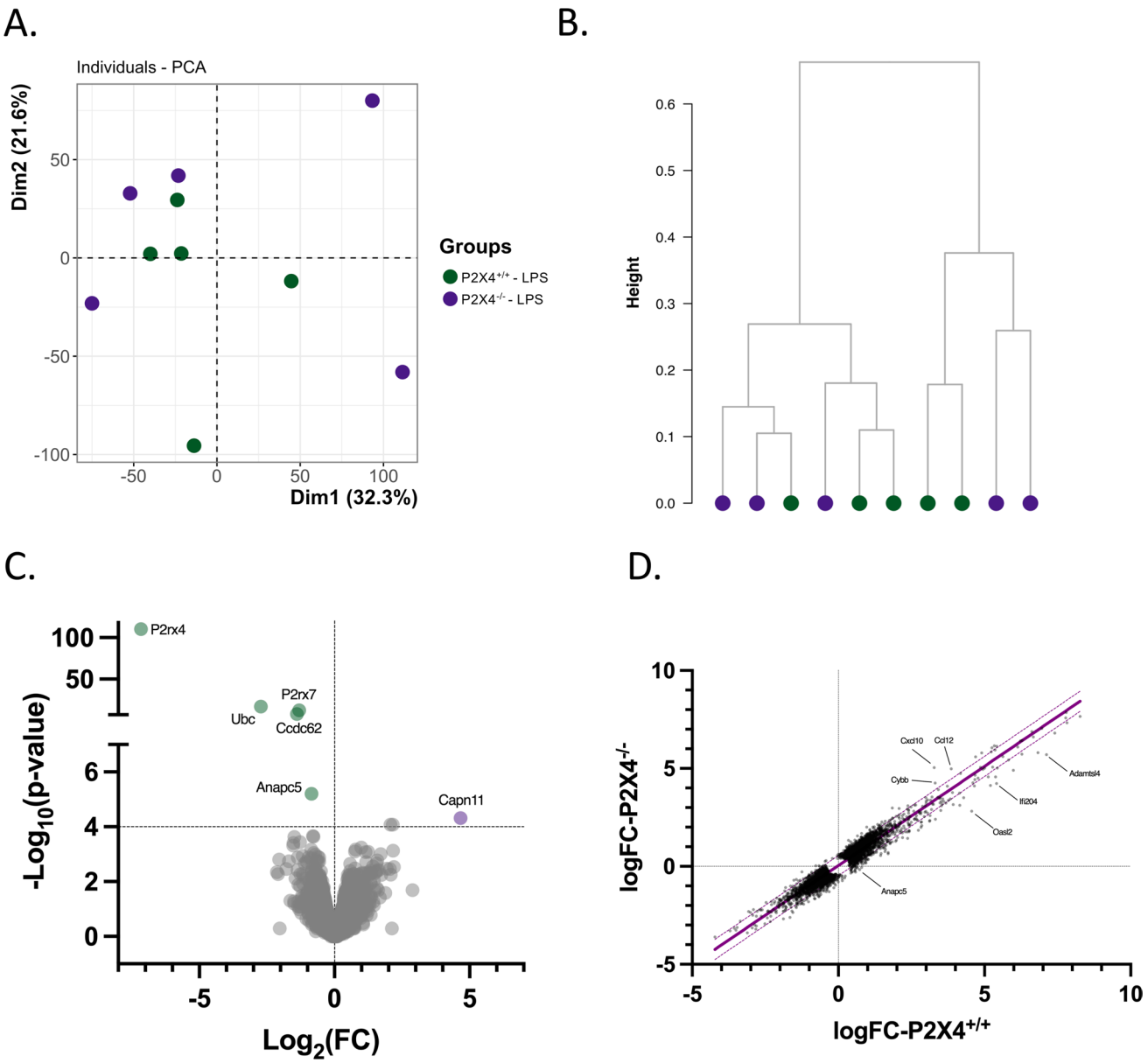

Fig. 3 Impact of *P2rx4* deficiency in reactive microglia. **A**. Principal component analysis of gene expression in $P2X4^{+/+}$ and $P2X4^{-/-}$ reactive microglia, based on the 10,788 expressed genes. **B**. Hierarchical clustering of gene expression in $P2X4^{+/+}$ and $P2X4^{-/-}$ reactive microglia, based on the 10,788 expressed genes. **C**. Volcano plot displaying the six genes that are deregulated (FDR < 0.1) in $P2X4^{-/-}$ compared to $P2X4^{+/+}$ reactive microglia. x-axis: log2 of fold-change in expression between $P2X4^{+/+}$and $P2X4^{-/-}$ reactive microglia. y-axis: $-\log_{10}$ of p value; the horizontal dotted line represents a p value = 10^{-4}, corresponding to FDR = 0.1. Dark green: down-regulated in $P2X4^{-/-}$. Dark purple: up-regulated in $P2X4^{-/-}$. **D**. Comparison of LPS-induced fold-change (FC) in $P2X4^{+/+}$ and $P2X4^{-/-}$ microglia. Each dot represents a gene which x/y coordinates correspond to FC in $P2X4^{+/+}$ (WT) and $P2X4^{+/+}$ (KO) respectively. The first bisector (plain purple line) represents equal FC in LPS-induced gene expression variations in $P2X4^{+/+}$ and $P2X4^{-/-}$. Dotted purple lines represent 95% interval confidence

contribution (that would remain non-significant in differential expression analysis), we performed GSEA analysis in reactive microglia isolated from either $P2X4^{+/+}$ or $P2X4^{-/-}$ mice. Despite analyzing several genes set categories of the Mouse MSigDB Collections, we only identified a weak enrichment of the "Wang response to bexarotene (up)" (i.e. Genes up-regulated in the mouse lung cancer model and which reverted to normal levels upon treatment with bexarotene) in the $P2X4^{-/-}$ reactive microglia (detailed results in Table S3).

Thus, DE and GSEA analyses show little if any contribution of P2X4 receptor to microglia reaction in this sepsis model. Yet, these two types of analyses do not consider the intensity of the changes, and we reasoned that P2X4 could

alter the intensity of gene deregulations but without affecting the pathways involved. We thus compared, for the DEGs in either and both $P2X4^{+/+}$ or $P2X4^{-/-}$ microglia, the measured fold-change. Figure 3D revealed that almost all DEGs exhibit comparable fold-change in both genotypes as shown by their proximity to the first bisector of the graph. Only a few genes slightly deviated, with for example *Cybb*, *Cxcl10* and *Ccl12* being more up-regulated in $P2X4^{-/-}$ microglia while *Oasl2*, *Ifi204* and *Adamtsl4* are less up-regulated. The detailed results of LPS-induced gene expression changes in $P2X4^{+/+}$ and $P2X4^{-/-}$ are shown in Table S4 (restricted to the ≈ 50% most expressed genes; i.e. log(cpm) > 4).

Finally, to assess whether *P2rx4* deficiency may affect specific microglia states already described in the literature, we calculated in each experimental condition the gene signature activity using the Z-score method [26]. More specifically, we assessed the Reactome [7], the conserved DIM (Disease Inflammatory Macrophages) and DAM (Disease Associated Microglia) [27], and the IAM (Inflammatory Associated Microglia) [28] signatures. As expected, LPS treatment affected both Reactome, IAM and DIM microglia signatures in $P2X4^{+/+}$ microglia (Fig. 4A–C). However, our analysis also revealed that *P2rx4* deficiency had no measured impact on these signatures. Of note, only the expression of *Spp1* from the DAM signature was altered after LPS administration. Importantly, it was affected similarly in WT and *P2rx4*-deficient microglia (Fig. 4D).

Overall, all of our analyses of the effects of P2X4 on the LPS-induced microglia reaction confirmed that this receptor had little, if any impact, on the remodeling of the microglia transcriptome in our mouse model of sepsis.

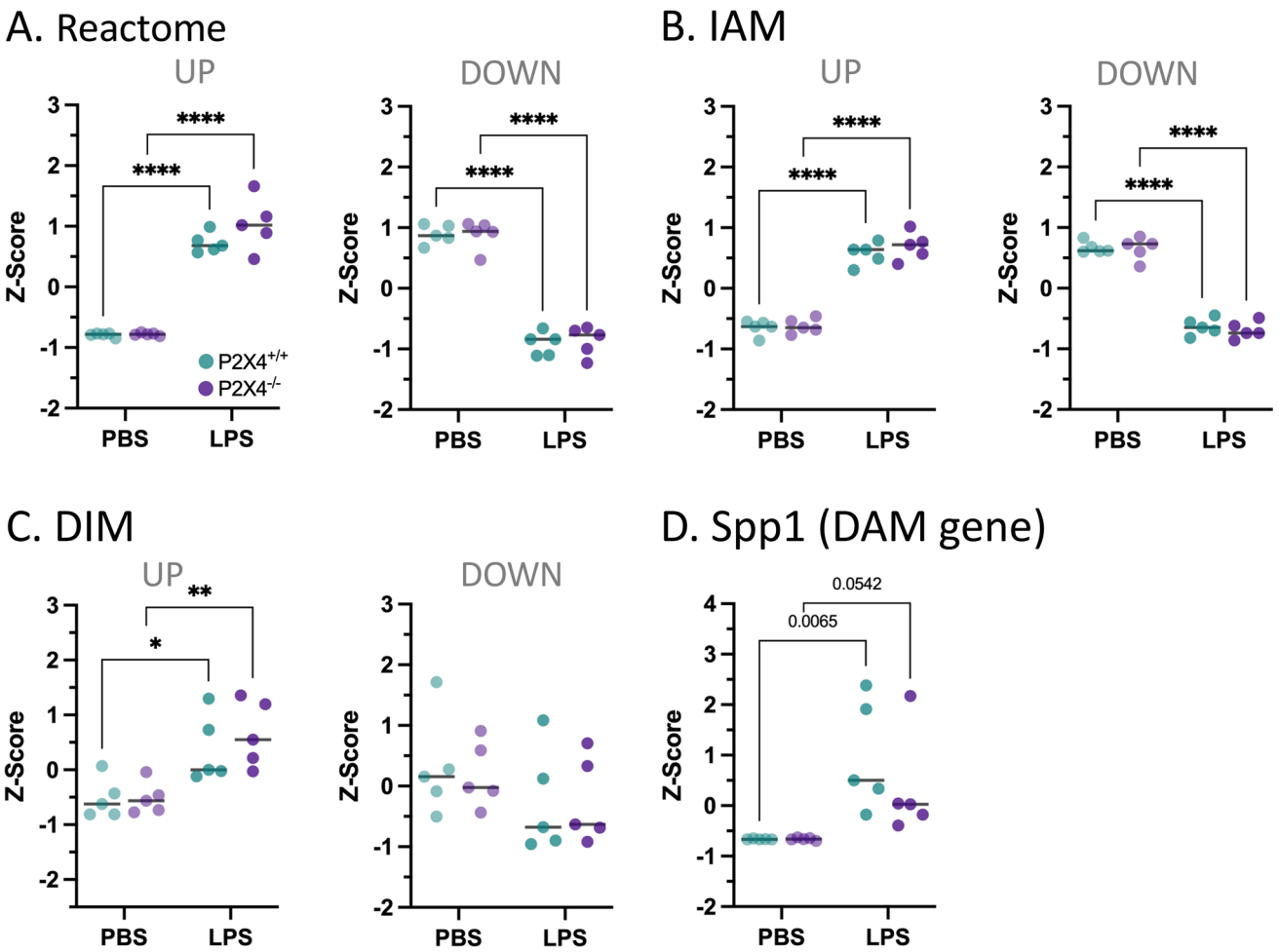

Fig. 4 Impact of *P2rx4* deficiency on specific microglia signatures. Plots indicating distribution of the signature activities in $P2X4^{+/+}$ and $P2X4^{-/-}$, homeostatic and reactive microglia. Each dot indicates the mean Z-score of the microglia sample for each signature. The signatures are activities of Reactome up- and down-regulated gene signatures **A**. IAM up- and down regulated gene signatures **B**. DIM up- and down-regulated gene signatures **C**. *Spp1* gene expression **D**. Statistics: two-way ANOVA with *LPS-Treatment* and *Genotype* as between subjects' factors; *LPS-treatment*: $p < 0.001$; FDR corrected post hoc tests LPS vs PBS: * $p < 0.05$; ** $p < 0.01$; **** $p < 0.0001$ or actual p values. Lines indicate the median Z-score

Discussion

Whether bacterial, viral, fungal or parasitic in origin, infections can lead to sepsis, a clinical syndrome characterized by a dysregulated host response to the infection [29]. Sepsis is life-threatening, and accumulating evidence suggests that sepsis survivors display long-term neurological sequelae, including cognitive impairment [30]. In the elderly, who, due to physiologic frailty and immune senescence, are more susceptible to infection, the prevalence of sepsis is increased and may affect the progression of neurodegenerative diseases, such as Alzheimer disease.

The pathogenesis of long-term cognitive impairment after sepsis is still poorly understood, but several mechanisms, including Blood–Brain Barrier (BBB) dysregulation, neuroinflammation, neurotransmitter dysfunction and neuronal loss are likely to play substantial roles [31]. Neuroinflammation is a major component of the pathogenesis of numerous neurological and neurodegenerative diseases, and microglia play a key role in the induction, the propagation and the maintenance of these neuroinflammatory processes [32]. Interestingly, it has been shown that inhibition of microglial reaction by minocycline can alleviate long-term memory impairment in mice with cecal ligation puncture, an animal model of sepsis [33], thus providing proof of principle that targeting microglia may represent a useful therapeutic strategy to prevent the adverse effects of the sickness behavior syndrome. Further, recent studies have highlighted that reactive microglia exist in different states, which can have either beneficial or detrimental impact on brain functioning [6]. Thus, modulating microglia reaction by interfering with important signalling pathways offers the theoretical opportunity to tune the microglial reaction towards beneficial functions for the disease outcome.

ATP plays a key role as danger signal mediating inflammation at the periphery and in the brain [34]. P2X receptors, which are ATP-gated ion channels, can efficiently sense ATP concentration changes. P2rX4 and P2rX7 are the main P2X receptors expressed in microglia, with P2rX4 showing at least 10 times higher affinity than P2rX7 for ATP [35]. Targeting P2rX4 receptors seems particularly interesting since, first it is highly permeable to calcium and has been shown to be involved in neuropathological processes [8, 13, 16, 36, 37], and second because it is virtually absent in homeostatic conditions but de novo expressed in reactive microglia [38]. Therefore, we hypothesized that targeting P2rX4 receptors may provide a mean to alter the microglia state and to redirect it towards a more protective, less inflammatory phenotype.

Consistent with its low expression in homeostatic microglia, our results demonstrate that *P2rx4* deficiency does not significantly affect the microglial cell biology in physiological conditions. This lack of impact is unlikely due to a lack of the sensitivity in the methods used as all approaches, including the sensitive GSEA one, led to the same conclusion. Further, as the $P2X4^{-/-}$ mice used are global knock-out, our results also highlight that absence of P2X4 receptors in neurons, oligodendrocytes and astrocytes, which also express P2X4 receptors, does not strongly impact on the brain functioning. Indeed, if this was the case one would expect that the transcriptome of microglia, which constantly monitors and senses the brain environment, would be affected. Of note, most of the genes (9/11) whose expressions are affected in $P2X4^{-/-}$ are located within 7.8 Mbase from the *P2rx4* gene on chromosome 5 [39]. It cannot therefore be ruled out that alterations in gene expression are due to the introduction of ß-galactosidase or the neomycin cassette, and to chromatin modification.

Our model of LPS-induced microglia reaction consisted in intraperitoneal administration of high dose of LPS and was associated with a sickness behavior syndrome characterized by important body weight loss. At the cellular level, it induces a strong remodeling of the microglia transcriptome as highlighted by the large number of deregulated genes (i.e. about 40% of the microglia expressed genes; [7]). Surprisingly, while *P2rx4* was indeed up-regulated in LPS-treated mice, we did not detect any coordinated effects of P2X4 deficiency on the LPS-induced microglia reactivity, and deregulated genes between $P2X4^{+/+}$ and $P2X4^{-/-}$ mice were the same in LPS-treated and control animals. Of note, even the very sensitive GSEA approach failed to identify any gene set significantly impacted by P2X4 deficiency.

These results are contrasting with those of Vazquez-Villoldo et al. [36] who showed that P2X4 receptors control the microglial survival. While the route of administration and doses match between the two studies (i.e. intraperitoneal administration of either 3 mg/kg (Vazquez-Villoldo study) or 4 mg/kg (present study)) there are other important differences between both studies. First, Vazquez-Villoldo used young adult male Lewis rats, whereas we used C57BL6/J young adult female mice; second, they investigated either the spinal cord or the dentate gyrus microglia, whereas we analyzed cortical microglia. It is known that the transcriptome and the general state of microglia differ depending on the species [40], the sex [41] and/or the brain area [42]. This may explain the difference observed between the two studies.

These results also contrast from results from our own lab showing an involvement of P2X4 receptors in the microglial response in either neuropathic pain [8] and in epilepsy [13]. The reasons for these differences are not clear but may indicate that microglial P2X4 receptors are

involved in microglia reaction only in case of intense stimuli or when neurodegeneration occurs. This is also consistent with the observation that in different neuropathological models, only a subset of reactive microglia are positive for *P2rX4* by immunohistochemistry [8, 13, 14].

Ubc and *Anapc5* are two genes involved in the control of ubiquitination and proteasome-mediated degradation [43, 44]. The strong *Ubc* down-regulation we observed in both homeostatic and reactive *P2X4*$^{-/-}$ microglia, as well as the blunting of LPS-mediated up-regulation of *Anapc5* in *P2X4*$^{-/-}$ microglia, suggests that P2X4 may be involved in the protein degradation both under physiological and pathological conditions. Complementary studies are however needed to further explore this hypothesis. Yet *Anapc5* and *Ubc* are located within 80 Kbase and 2.6 Mbase from *P2rx4* on chromosome 5, respectively, suggesting that the presence of the ß-galactosidase and neomycin cassette can alter the expression of a subset of nearby genes.

Overall, although negative our results highlight that P2X4 receptors do not represent a universal target to modulate microglia reaction. On the opposite, targeting P2X4 receptors might be relevant to specific neuropathological conditions. Whether microglial P2X4 receptors are mobilized only under neurodegenerative conditions needs to be investigated in further studies.

Supplementary Information The online version contains supplementary material available at https://doi.org/10.1007/s11302-023-09984-5

Acknowledgements We thank Duperray C for their help in flow cytometry; Dubois E & Rialle S (MGX platform) and Lachuer J (ProfilExpert) for useful discussion on RNA-seq analyses; Dr Vincent Compan for reviewing the manuscipt.

Author contribution PN performed animal treatments, histological analyses, microglia sorting, RNA extraction and helped prepare the figures; LU contributed to the initial scientific discussions; FR funded the study and was a major contributor in its design; HH performed all the bioinformatic analyses, prepared the figures and wrote the manuscript. All authors reviewed the manuscript.

Funding This work was funded by the Fonds Unique Interministeriel FUI DiaTrAL (Diagnostic et Traitements de la maladie d'Alzheimer) and the Labex ICST [ANR 11-LABX-0015].

Data Availability Upon acceptance of the manuscript, raw sequencing data that support the findings of this study will be deposited onto the NCBI Gene Expression Omnibus.

Declarations

Competing interests The authors declare no competing interests.

Ethical approval All experiments followed European Union (Council directive 86/609EEC) and institutional guidelines for the care and use of laboratory animals. The animal experiment protocols used in this study were approved by the Comité d'Ethique pour l'Expérimentation Animale Languedoc Roussillon (CEEA-LR; APAFiS#5253).

References

1. Iskander KN, Osuchowski MF, Stearns-Kurosawa DJ et al (2013) Sepsis: multiple abnormalities, heterogeneous responses, and evolving understanding. Physiol Rev 93(3):1247–1288. https://doi.org/10.1152/physrev.00037.2012
2. Calovi S, Mut-Arbona P, Sperlagh B (2019) Microglia and the purinergic signaling system. Neuroscience 405:137–147. https://doi.org/10.1016/j.neuroscience.2018.12.021
3. Farber K, Kettenmann H (2006) Purinergic signaling and microglia. Pflugers Arch 452(5):615–621 (Epub 2006 Jun 21)
4. Schedlowski M, Engler H, Grigoleit JS (2014) Endotoxin-induced experimental systemic inflammation in humans: a model to disentangle immune-to-brain communication. Brain Behav Immun 35:1–8. https://doi.org/10.1016/j.bbi.2013.09.015
5. Wolf SA, Boddeke HW, Kettenmann H (2017) Microglia in physiology and disease. Annu Rev Physiol 79:619–643. https://doi.org/10.1146/annurev-physiol-022516-034406
6. Paolicelli RC, Sierra A, Stevens B et al (2022) Microglia states and nomenclature: a field at its crossroads. Neuron 110(21):3458–3483. https://doi.org/10.1016/j.neuron.2022.10.020
7. Hirbec H, Marmai C, Duroux-Richard I et al (2018) The microglial reaction signature revealed by RNAseq from individual mice. Glia 66(5):971–986. https://doi.org/10.1002/glia.23295
8. Ulmann L, Hatcher JP, Hughes JP et al (2008) Up-regulation of P2X4 receptors in spinal microglia after peripheral nerve injury mediates BDNF release and neuropathic pain. J Neurosci 28(44):11263–11268
9. Tsuda M, Shigemoto-Mogami Y, Koizumi S et al (2003) P2X4 receptors induced in spinal microglia gate tactile allodynia after nerve injury. Nature 424(6950):778–783. https://doi.org/10.1038/nature01786
10. Haynes SE, Hollopeter G, Yang G et al (2006) The P2Y12 receptor regulates microglial activation by extracellular nucleotides. Nat Neurosci 9(12):1512–1519
11. Antonioli L, Blandizzi C, Fornai M et al (2019) P2X4 receptors, immunity, and sepsis. Curr Opin Pharmacol 47:65–74. https://doi.org/10.1016/j.coph.2019.02.011
12. Coull JA, Beggs S, Boudreau D et al (2005) BDNF from microglia causes the shift in neuronal anion gradient underlying neuropathic pain. Nature 438(7070):1017–1021. https://doi.org/10.1038/nature04223
13. Ulmann L, Levavasseur F, Avignone E et al (2013) Involvement of P2X4 receptors in hippocampal microglial activation after status epilepticus. Glia 61(8):1306–1319. https://doi.org/10.1002/glia.22516
14. Hua J, Garcia de Paco E, Linck N et al (2023) Microglial P2X4 receptors promote ApoE degradation and contribute to memory deficits in Alzheimer's disease. Cell Mol Life Sci 80(5):138. https://doi.org/10.1007/s00018-023-04784-x
15. Jung S, Aliberti J, Graemmel P et al (2000) Analysis of fractalkine receptor CX(3)CR1 function by targeted deletion and green fluorescent protein reporter gene insertion. Mol Cell Biol 20(11):4106–4114
16. Ulmann L, Hirbec H, Rassendren F (2010) P2X4 receptors mediate PGE2 release by tissue-resident macrophages and initiate inflammatory pain. Embo J 29(14):2290–2300
17. Philippe N, Salson M, Commes T et al (2013) CRAC: an integrated approach to the analysis of RNA-seq reads. Genome Biol 14(3):R30. https://doi.org/10.1186/gb-2013-14-3-r30
18. Liao Y, Smyth GK, Shi W (2014) featureCounts: an efficient general purpose program for assigning sequence reads to genomic features. Bioinformatics 30(7):923–930. https://doi.org/10.1093/bioinformatics/btt656

19. Robinson MD, McCarthy DJ, Smyth GK (2010) edgeR: a Bioconductor package for differential expression analysis of digital gene expression data. Bioinformatics 26(1):139–140. https://doi.org/10.1093/bioinformatics/btp616
20. Le S, Josse J, Husson F (2008) FactoMineR: an R package for multivariate analysis. J Stat Softw 25(1):1–18. https://doi.org/10.18637/jss.v025.i01
21. Ogata H, Goto S, Sato K et al (1999) KEGG: Kyoto encyclopedia of genes and genomes. Nucleic Acids Res 27(1):29–34. https://doi.org/10.1093/nar/27.1.29
22. Jassal B, Matthews L, Viteri G et al (2020) The reactome pathway knowledgebase. Nucleic Acids Res 48(D1):D498–D503. https://doi.org/10.1093/nar/gkz1031
23. Subramanian A, Tamayo P, Mootha VK et al (2005) Gene set enrichment analysis: a knowledge-based approach for interpreting genome-wide expression profiles. Proc Natl Acad Sci U S A 102(43):15545–15550. https://doi.org/10.1073/pnas.0506580102
24. Bechade C, D'Andrea I, Etienne F et al (2021) The serotonin 2B receptor is required in neonatal microglia to limit neuroinflammation and sickness behavior in adulthood. Glia 69(3):638–654. https://doi.org/10.1002/glia.23918
25. Zhang Y, Chen K, Sloan SA et al (2014) An RNA-sequencing transcriptome and splicing database of glia, neurons, and vascular cells of the cerebral cortex. J Neurosci 34(36):11929–11947. https://doi.org/10.1523/JNEUROSCI.1860-14.2014
26. Levine DM, Haynor DR, Castle JC et al (2006) Pathway and gene-set activation measurement from mRNA expression data: the tissue distribution of human pathways. Genome Biol 7(10):R93. https://doi.org/10.1186/gb-2006-7-10-r93
27. Silvin A, Uderhardt S, Piot C et al (2022) Dual ontogeny of disease-associated microglia and disease inflammatory macrophages in aging and neurodegeneration. Immunity. 55(8):1448-1465 e6. https://doi.org/10.1016/j.immuni.2022.07.00
28. Sousa C, Golebiewska A, Poovathingal SK, et al. (2018) Single-cell transcriptomics reveals distinct inflammation-induced microglia signatures. EMBO Rep 19(11) https://doi.org/10.15252/embr.201846171
29. Cecconi M, Evans L, Levy M et al (2018) Sepsis and septic shock. Lancet 392(10141):75–87. https://doi.org/10.1016/S0140-6736(18)30696-2
30. Iwashyna TJ, Ely EW, Smith DM et al (2010) Long-term cognitive impairment and functional disability among survivors of severe sepsis. JAMA 304(16):1787–1794. https://doi.org/10.1001/jama.2010.1553
31. Li Y, Ji M, Yang J (2022) Current Understanding of long-term cognitive impairment after sepsis. Front Immunol 13:855006. https://doi.org/10.3389/fimmu.2022.855006
32. Deczkowska A, Keren-Shaul H, Weiner A et al (2018) Disease-associated microglia: a universal immune sensor of neurodegeneration. Cell 173(5):1073–1081. https://doi.org/10.1016/j.cell.2018.05.003
33. Michels M, Vieira AS, Vuolo F et al (2015) The role of microglia activation in the development of sepsis-induced long-term cognitive impairment. Brain Behav Immun 43:54–59. https://doi.org/10.1016/j.bbi.2014.07.002
34. Rodrigues RJ, Tome AR, Cunha RA (2015) ATP as a multi-target danger signal in the brain. Front Neurosci 9:148. https://doi.org/10.3389/fnins.2015.00148
35. Khakh BS, North RA (2012) Neuromodulation by extracellular ATP and P2X receptors in the CNS. Neuron 76(1):51–69. https://doi.org/10.1016/j.neuron.2012.09.024
36. Vazquez-Villoldo N, Domercq M, Martin A et al (2014) P2X4 receptors control the fate and survival of activated microglia. Glia 62(2):171–184. https://doi.org/10.1002/glia.22596
37. Avignone E, Ulmann L, Levavasseur F et al (2008) Status epilepticus induces a particular microglial activation state characterized by enhanced purinergic signaling. J Neurosci 28(37):9133–9144
38. Toulme E, Garcia A, Samways D et al (2010) P2X4 receptors in activated C8–B4 cells of cerebellar microglial origin. J Gen Physiol 135(4):333–353. https://doi.org/10.1085/jgp.200910336
39. Sim JA, Chaumont S, Jo J et al (2006) Altered hippocampal synaptic potentiation in P2X4 knock-out mice. J Neurosci 26(35):9006–9009
40. Sharma K, Bisht K, Eyo UB (2021) A comparative biology of microglia across species. Front Cell Dev Biol 9:652748. https://doi.org/10.3389/fcell.2021.652748
41. Han J, Fan Y, Zhou K et al (2021) Uncovering sex differences of rodent microglia. J Neuroinflammation 18(1):74. https://doi.org/10.1186/s12974-021-02124-z
42. Grabert K, Michoel T, Karavolos MH et al (2016) Microglial brain region-dependent diversity and selective regional sensitivities to aging. Nat Neurosci 19(3):504–516. https://doi.org/10.1038/nn.4222
43. Bianchi M, Giacomini E, Crinelli R et al (2015) Dynamic transcription of ubiquitin genes under basal and stressful conditions and new insights into the multiple UBC transcript variants. Gene 573(1):100–109. https://doi.org/10.1016/j.gene.2015.07.030
44. Castro A, Bernis C, Vigneron S et al (2005) The anaphase-promoting complex: a key factor in the regulation of cell cycle. Oncogene 24(3):314–325. https://doi.org/10.1038/sj.onc.1207973

Publisher's Note Springer Nature remains neutral with regard to jurisdictional claims in published maps and institutional affiliations.

Springer Nature or its licensor (e.g. a society or other partner) holds exclusive rights to this article under a publishing agreement with the author(s) or other rightsholder(s); author self-archiving of the accepted manuscript version of this article is solely governed by the terms of such publishing agreement and applicable law.

Paola Nobili got her PhD in Translational and Molecular Medicine in Italy, at the university of Milan.She is currently post-doctoral researcher at the Institute of Functional Genomics (IGF) in Montpellier (France), where she is studying the role of extracellular purines and purinergic receptors in both physiological and pathological conditions, working on rodent models.She worked for several years in neuroscience field and she developed a deep interest in better understanding the mechanism underlying pathological processes and in identifying possible therapeutical strategies to implement treatment options.